CHAPTER

Body-on-a-chip systems: Design, fabrication, and applications

11

Mandy B. Esch*, Gretchen J. Mahler†

Center for Nanoscale Science and Technology, National Institute of Standards and Technology, Gaithersburg, MD, United States Department of Biomedical Engineering, Binghamton University, Binghamton, NY, United States†*

1 INTRODUCTION

The discovery and development of new drugs is a long, research-intensive, and costly process. Bringing a new drug to market takes an average of 10–12 years and, if linking the expenditures for abandoned compounds to those that are approved and including both small molecules and biologics, costs $1.3–2.6 billion USD [1]. A report from the Centers for Medical Research (CMR) [2] shows that <1 out of every 10 drugs entering clinical trials makes it to market. Most of these compounds fail due to the lack of efficacy [2]. Both the expense of testing new drugs and the large number of new compounds available to be tested make a rapid, inexpensive method for accurately assessing efficacy and toxicity in humans essential in the pharmaceutical industry.

Animal studies are the primary method used to determine toxicological and pharmacological profiles, but animal experiments can take months to complete and are costly, and animal drug metabolism can differ substantially from human metabolism. Cytochrome P450 (CYP450) enzyme isoform composition, expression, and activity differ between animal species, for example [3]. For every 50 drugs that are safe for use in animals, approximately one drug proves safe for use in humans [4,5]. This is an ethical dilemma, not only for the use of animals but also for the human patients involved in clinical trials.

In vitro cell culture systems are widely used as an experimental tool during the preclinical phase. Human cells from a single organ or tissue are generally cultured in multiwell plates in 2-D conditions, which are easy to manipulate and allow for high-throughput assays. Cell cultures are limited in their ability to predict drug toxicity and efficacy, however, and one of the primary reasons for this is a lack of physiological relevance [6]. Two dimensional, single-cell-type cell cultures cannot recreate the in vivo microenvironment, including cell-cell and cell-matrix interactions;

nutrient and oxygen supply; metabolite and waste removal; and, most importantly, direct interaction with other organs and tissues or interactions through soluble proteins or metabolites [7].

Microfabrication and microfluidic technologies have enabled the creation of body-on-a-chip devices that provide physiologically relevant microenvironments for and interactions between human cells. Body-on-a-chip systems replicate human physiology with respect to the size relationships of organs, blood distribution, and blood flow. When operated with human-derived cells, these systems are capable of simulating human drug metabolism and subsequent therapeutic actions, toxic side effects, and tissue-specific functional response. Body-on-a-chip devices have the potential to direct drug development toward the most promising candidates or help other drug candidates "fail faster" or be removed from the new drug pipeline before human clinical trials. The goal of this chapter is to provide an overview of the current state of body-on-a-chip technology, including chip design principles, body-on-a-chip fabrication considerations, and current applications of the technology.

2 A PRIMER ON BODY-ON-A-CHIP SYSTEMS

2.1 BODY-ON-A-CHIP DEVICES AND PBPK MODELS

Body-on-a-chip devices are physical representations of physiologically based pharmacokinetic (PBPK) models. PBPK models are mathematical models of human metabolism that take into account physiological parameters such as organ sizes, blood flow rates through organs, and enzyme activity. To develop PBPK models, the human body is first represented as a drawing that shows organs as boxes and blood flow as arrows (see Fig. 1). Often, the human body is simplified so that the drawing only contains organs and reactions that are relevant for the metabolism of a particular drug. Organs that do not absorb the drug or do not otherwise contribute to its metabolism are left out. These simplified drawings can be used to develop body-on-a-chip devices.

PBPK drawings can guide the layout of microfluidic body-on-a-chip systems in the following way: Each box (i.e., each organ) becomes a cell culture chamber on the chip, and each arrow (i.e., blood flow) becomes a microfluidic channel. The sizes of the cell culture chamber are determined by the size of the organ in the human body and the density of the engineered tissue construct that will represent that organ (see Section 2.2 for detailed calculations). If all tissue constructs have the same cell density, then all organ chambers can be scaled using the same scaling factor. Second, the sizes of microfluidic channels are determined by the amount of flow that is needed to perfuse the organ chamber at the same rate as the same volume of tissue is perfused inside the body. Both organ chamber sizes and microfluidic channel sizes are designed to mimic conditions in the body. The overall arrangement of organ chambers and microfluidic channels will match that of PBPK drawing, simplifying the human body. Abaci and Shuler [8] have written a useful guide to the design of PBPK-based microphysiological platforms.

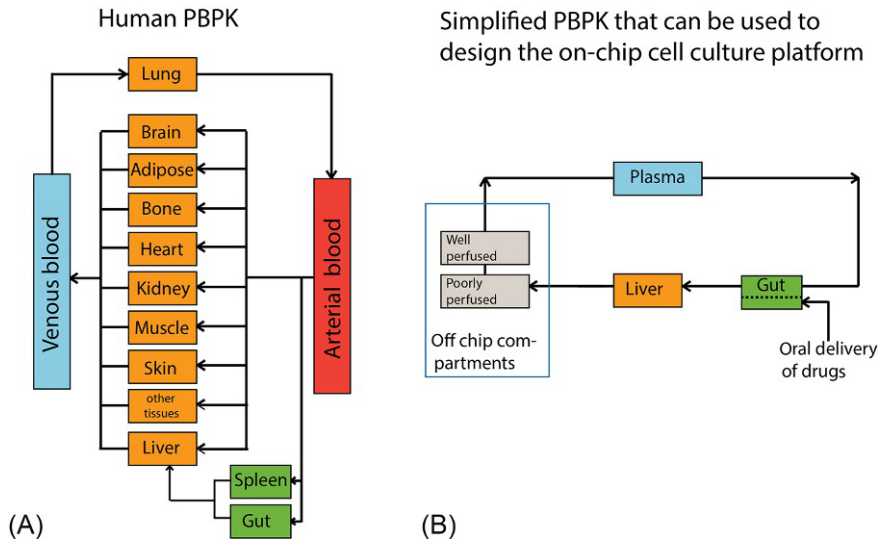

FIG. 1

A schematic of a PBPK model of the human body and of a simplified version of the human body that can be used to build a body-on-a-chip device.

The biggest challenge developers of body-on-a-chip devices face is that it is difficult to represent the entire human body with a microfluidic system. There are many organs that are interconnected with each other and that have their own microarchitecture, consisting of organ-specific structures and many different cell types. There are also systems that respond to varying conditions, such as the immune system and the endocrine signaling system. In addition, even if it is possible to create a system that represents all the complexities of the human body, it is quite likely that such a device would be difficult to use. Introducing simplifications is necessary to achieve workable proof-of-concept devices.

What kind of simplifications can reasonably be made depends on the question that will be investigated with the device. For example, Mahler et al. asked the question whether the bioavailability of acetaminophen can be replicated with a body-on-a-chip system [9]. The concentration of acetaminophen immediately after ingestion (and before the drug is circulated throughout the body, metabolized, and excreted) is determined by the rate of transport across the intestinal epithelium and the rate of first-pass metabolism in the GI tract and the liver. A system that contains those two organs and the appropriate amount of liquid (i.e., the appropriate amount of liquid surrogate to represent the body's blood) can be used to estimate the acetaminophen blood concentration immediately after ingestion. A simplified system as described is easier to work with than a complex device with many organ compartments, yet it can still give an answer to the question of how much acetaminophen reaches the systemic circulation after ingestion.

When simplifying a body-on-a-chip system by excluding organs, it is important to include the liquid portions of those excluded organs and the full amount of blood. That strategy ensures that the system has a physiological liquid-to-cell or fluid-to-tissue ratio and that drug and metabolite concentrations are similar to what they would be inside the body. Since both drug efficacy and drug toxicity can strongly depend on drug and metabolite concentrations, it is vital to pay close attention to the amount of liquid within the body-on-a-chip system.

Another consideration when designing body-on-a-chip systems is the scaling factor that will be used to determine the sizes of organ chambers. There should be a minimum number of cells that represent an organ, and the scaling factor will vary from system so system depending on the smallest organ that will be included. Some organs, such as lymph nodes, are very small compared with other organs. If those small glands play an important role in the drug metabolism to be studied, then they need to be represented with a minimum number of cells that will produce measurable reactions. All other organs of the system need to be scaled so that their size reflects the correct physiological size ratio.

Sometimes, the need to make simplifications arises from the technology used to create the body-on-a-chip device. For example, a gut module with an apical and a basolateral chamber could be machined in plastic (instead of silicon) and become an off-chip component. It might technically be easier to connect such an off-chip component directly to the liver, instead of splitting its output between the liver and the systemic circulation. When making such simplification, the original PBPK drawing can be redrawn to reflect it (see Fig. 1B).

When body-on-a-chip devices are developed using this strategy, they become physical representation of the PBPK model, where enzymatic reactions taking place within the organ compartments replace equations and actual fluidic flow through interconnecting microfluidic channels replaces fluid flow equations. This relationship becomes useful because we are able to build a very accurate PBPK model of the body-on-a-chip device [10]. That model will be quite accurate because we know many of the needed parameters, such as the sizes of cell culture chambers, cell density within a tissue, and liquid flow rates. We also know which simplifications we have made, that is, which functions of the human body will not be present in the device.

We can now use the devices in combination with the PBPK models to obtain parameters that cannot be obtained otherwise, for example, the rate of first-pass metabolism of acetaminophen, and other parameters that describe its absorption, distribution, metabolism, and excretion (ADME). It is also possible that single tissue-on-a-chip devices such as those reviewed by Bhise et al. [11] can, in conjunction with their mathematical models, can be used to obtain tissue-specific parameters that were previously unknown [8]. We can also use the system to test assumptions we make, and those assumptions can be validated. Through an iterative process, both the devices and the accompanying PBPK model can be refined, so that eventually the model will predict the outcome of an experiment with the body-on-a-chip device accurately. Those parameters can then be used to more accurately build PBPK models of more complex body-on-a-chip devices and of the human body (Fig. 2).

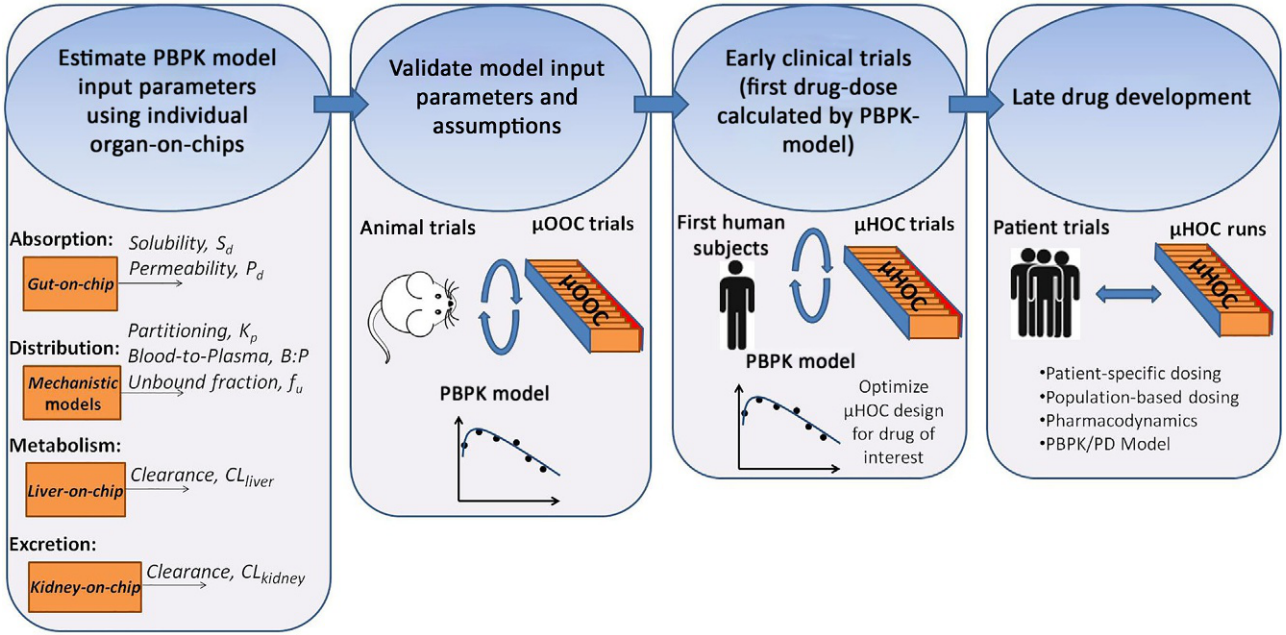

FIG. 2

Obtaining tissue-specific parameters with body-on-a-chip devices and integrating them to construct more accurate PBPKs.

Reproduced with permission from Abaci HE, Shuler ML. Human-on-a-chip design strategies and principles for physiologically based pharmacokinetics/pharmacodynamics modeling. Integr Biol 2015;7(4):383–91, the Royal Society of Chemistry.

Despite the initial simplifications body-on-a-chip developers make, devices that represent the human body fairly completely will remain the main goal. The more complex the body-on-a-chip system becomes, that is, the more organs are included and the more accurate flow rates and fluid residence times are achieved, the more the PBPK model of the device will resemble the PBPK model of the human body. Data that are produced with well-designed body-on-a-chip devices that represent the human body well will then indicate more reliably how a drug will behave inside the human body. In other words, the in vitro to in vivo conversion of the experimental outcome obtained from body-on-a-chip devices will be much easier to do and will be more accurate.

2.2 BODY-ON-A-CHIP DESIGN

Fluid dynamics and transport phenomenon equations can be used to design microfluidic body-on-a-chip systems. The flow inside a microfluidic channel can be analyzed by solving Navier-Stokes equation, assuming an incompressible fluid. The key component in body-on-a-chip design is equalizing the pressure drop across all interconnected channels and chambers to allow for a passive on-chip fluid flow split. The pressure drop across a fluidic channel is analogous to an electric circuit. Ohm's law relates the change in electric potential (ΔV) to the current I with $\Delta V = IR$. R, the resistance, is dependent on factors including the system and materials [12]. In microfluidic systems with a pressure difference (ΔP) across a fluid-filled channel, there is a flow rate (Q with units of volume/time) with $\Delta P = QR_H$. R_H is the hydrodynamic resistance, which is a function of the channel geometry and fluid viscosity [12]. The following equations were used to design the body chip shown in Fig. 3. The prototype was designed on the basis of the following constraints, which were first outlined by Sin et al. [14]:

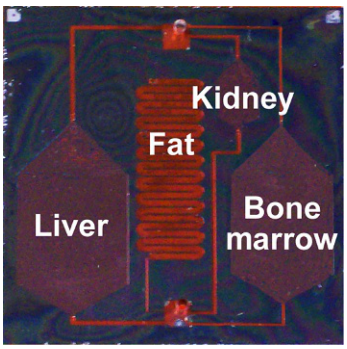

FIG. 3

Body-on-a-chip used by Mahler et al. [9] and Esch et al. [13] for first-pass metabolism studies.

Adapted from Mahler GJ, Esch MB, Glahn RP, Shuler ML. Characterization of a gastrointestinal tract microscale cell culture analog used to predict drug toxicity. Biotechnol Bioeng 2009;104(1):193–205.

(1) The ratio of the chamber sizes and the liquid residence times in each compartment should be physiologically realistic.
(2) Each chamber should have a minimum of 10^4 cells to facilitate analysis of chemicals.
(3) The hydrodynamic shear stress on the cells in tissue compartments should be within physiological values (<0.2 N/m^2 (<2 dyn/cm^2)). Much higher shear stress values are found in the vasculature; shear stress ranges in magnitude from 0.1 N/m^2 (1 dyn/cm^2) to 0.6 N/m^2 (6 dyn/cm^2) in venous vessels and from 1 N/m^2 (10 dyn/cm^2) to 7 N/m^2 (70 dyn/cm^2) in arterial vessels, and models of the vasculature can be included in these systems [15,16].
(4) The liquid-to-cell ratio should be close to the physiological value (1:2).

The channels are where fluid flows between chambers and into and out of the chip. Chambers are where cells are seeded onto the body-on-a-chip. These design calculations begin by defining the density (ρ), kinematic viscosity (ν), and dynamic viscosity (μ) of the circulating culture medium at 37°C. In addition, the height (h_{cl}) and diameter (d_{cl}) of cells should be estimated, and the number (N_{ch}), width (w_{ch}), length (l_{ch}), and height or depth (h_{ch}) of chambers should be determined. Cell area and volume can be estimated by defining the diameter of a cell (d_{cl}) and the height of a cell (h_{cl}) and assuming a cylindrical geometry:

$$\text{Cell area} = \frac{\pi * d_{cl}^2}{4} \left(\mu m^2\right) \tag{1}$$

$$\text{Cell volume} = \frac{\pi * d_{cl}^2 * h_{cl}}{4} \left(\mu m^3\right) \tag{2}$$

Equations in this chapter are valid in any consistent set of units. We specify one set in square braces for illustration. The total number of cells per chamber, assuming 100% confluency, can be also calculated:

$$\text{Number of cells per chamber} = N_c = \frac{4 * w_{ch} * l_{ch}}{\pi * d_{cl}^2} \tag{3}$$

Next, the desired flow rate through each chamber (Q_{ch}) should be defined. The flow rate through each chamber can be adjusted to provide a physiological shear stress to the cells seeded within each chamber. The total flow rate through all chambers should match the total pressure-driven flow rate from the peristaltic pump (Q_{total}). With chamber dimensions and flow rate through each chamber defined, the linear velocity, residence time, shear stress per unit area on cells, hydraulic diameter, and Reynolds number for each chamber can be calculated. Assumptions include an incompressible Newtonian fluid, a constant cross-sectional flow area, $h \ll w$ for the rectangular chambers and channels, a parabolic flow profile (fluid velocity is the fastest at the center and slowest near the channel wall), and no slip (zero velocity) at the walls. Equations have been simplified to their one-dimensional form:

$$\text{Chamber average velocity} = u_{ch} = \frac{Q_{ch}}{(h_{ch} - h_{cl}) * w_{ch}} \left(\mu m/s\right) \tag{4}$$

$$\text{Chamber residence time} = \frac{w_{ch}{}^{*}l_{ch}{}^{*}(h_{ch}-h_{cl})}{Q_{ch}}\ (\text{s}) \tag{5}$$

Physiological values for shear stress are generally $<0.2\ \text{N/m}^2$ ($<2\ \text{dyn/cm}^2$) for tissues, from $0.1\ \text{N/m}^2$ ($1\ \text{dyn/cm}^2$) to $0.6\ \text{N/m}^2$ ($6\ \text{dyn/cm}^2$) in venous vessels, and from $1\ \text{N/m}^2$ ($10\ \text{dyn/cm}^2$) to $7\ \text{N/m}^2$ ($70\ \text{dyn/cm}^2$) in arterial vessels [15–17]. Shear rate at the inner wall of a Newtonian fluid flowing within a pipe can be described as

$$\text{Shear rate} = \gamma = \frac{8{}^{*}u_{ch}}{(h_{ch}-h_{cl})}\ (1/\text{s}) \tag{6}$$

The shear stress (τ) can be calculated by multiplying the shear rate (γ) by the dynamic viscosity of the fluid:

$$\text{Shear stress per unit area on cells} = \tau = \gamma{}^{*}\mu\ \left(\text{N/cm}^2\right) \tag{7}$$

Shear stress can also be estimated using the standard equation for wall shear stress for Poiseuille (pressure-driven) flow in a rectangular channel:

$$\tau = \frac{6{}^{*}Q_{ch}{}^{*}\mu}{(h_{ch}-h_{cl})}\ \left(\text{N/cm}^2\right) \tag{8}$$

The hydraulic diameter (D_H) or characteristic length of the chambers is needed to calculate the Reynolds number in noncircular channels and is equal to four times the area of flow divided by the perimeter of the duct in contact with fluid:

$$\text{Hydraulic diameter} = D_H = \frac{2{}^{*}w_{ch}{}^{*}(h_{ch}-h_{cl})}{w_{ch}+(h_{ch}-h_{cl})}\ (\mu\text{m}) \tag{9}$$

Next, the dimensionless Reynolds number (Re) is calculated using the hydraulic diameter to determine if flow is turbulent or laminar. Flow is laminar if $Re < 2300$, transient for $2300 < Re < 4000$, and turbulent if $Re > 4000$ [18]:

$$\text{Chamber Reynolds number} = Re = \frac{\rho{}^{*}u_{ch}{}^{*}D_H}{\mu} \tag{10}$$

In microfluidic devices, pressure-driven flow through channels and chambers is most often laminar [19]. Because the Reynolds number is usually very low, most of the pressure drop through the device is due to friction. To determine the pressure drop in the chambers, the friction factor is needed. To estimate the friction factor in the microfluidic chambers, the equation for the Darcy friction factor, f, for laminar flow in a circular pipe can be used [20]:

$$f = \frac{64}{Re} \tag{11}$$

The pressure drop through each chamber can then be determined using the Darcy-Weisbach equation:

$$\Delta P_{ch} = \frac{f{}^{*}\rho{}^{*}l_{ch}{}^{*}u_{ch}^2}{2{}^{*}D_H}\ (\text{Pa}) \tag{12}$$

In the example case, the chamber where cells were seeded had triangular distributors containing evenly spaced, 100 μm wide by 30 μm high posts or baffles to help

mix liquid at the chamber inlet and outlet. These baffles were previously found to more evenly distribute fluid flow throughout the chambers [14]. The pressure drop through the distributors was calculated with the Ergun equation [21], which describes flow through a packed bed and requires the following parameters to be defined:

$$\text{Width of baffles} = w_{baf}\ (\mu\text{m})$$

$$\text{Height of baffles} = h_{baf}\ (\mu\text{m})$$

$$\text{Width of distributor inlet} = w_{dist-in}\ (\mu\text{m})$$

$$\text{Void fraction} = \varepsilon = 0.75$$

$$\text{Length of inlet distributor} = l_{dist-in} = 0.5{*}w_{ch}\ (\text{mm})$$

$$\text{Volume of inlet distributor} = V_{dist-in} = \varepsilon{*}l_{dist-in}{*}w_{baf}{*}h_{baf}\ (\mu\text{L})$$

The distributors are not straight channels; therefore, there is a dependence of velocity on length. The following equations were derived from the Ergun equation for a right triangular entrance:

$$A = \frac{150{*}Q_{ch}{*}(1-\varepsilon)^2{*}\mu}{\varepsilon^3{*}w_{baf}^2{*}h_{baf}}\ \left(\text{mg}/\left(\mu\text{m s}^2\right)\right) \tag{13}$$

$$B = \frac{1.75{*}Q_{ch}^2{*}(1-\varepsilon){*}\rho}{\varepsilon^3{*}w_{baf}{*}h_{baf}^2}\ \left(\text{mg}/\text{s}^2\right) \tag{14}$$

The pressure drop through the inlet distributors was then calculated using.

$$\Delta P_{dist-in} = A{*}\ \ln\left(\frac{l_{dist-in}+w_{dist-in}}{w_{dist-in}}\right) - B{*}\left(\frac{1}{l_{dist-in}+w_{dist-in}} - \frac{1}{w_{dist-in}}\right)\ (\text{Pa}) \tag{15}$$

The chamber outlet distributors do not have baffles or cells and are shorter, isosceles (30°/30°/120°) triangles with a trimmed top. To calculate the pressure drop through the outlet distributors, the Darcy-Weisbach equation was used. The width of the channels connecting the chip inlet, chambers, and outlet remains constant, so the width of the channel leaving the distributor is the same as the inlet channel width ($w_{dis-in} = w_{dis-out}$). The width of the distributor changes over the distance from the chamber holding cells to the outlet channel, however, meaning that the hydraulic diameter changes with length. The pressure drop can be calculated by first defining the width of the exit channels and then by determining the length of the distributor using trigonometric definitions. Note that the length is corrected for the trimmed top of the isosceles triangle in Eq. (17):

$$\text{Width of the exit channel} = w_{dist-out} = w_{dist-in}$$

$$\text{Length of outlet distributor} = l_{out} = \frac{\frac{w_{ch}}{2}}{\tan\left(\frac{\pi}{3}\right)} \tag{16}$$

Correcting for the trimmed triangle top:

$$\text{Corrected length of outlet distributor} = l_{dist-out} = l_{out} - \frac{\frac{w_{dist-out}}{2}}{\tan\left(\frac{\pi}{3}\right)} \tag{17}$$

$$\text{Volume of outlet distributor} = \frac{w_{ch}{*}h_{ch}{*}l_{dist-out}}{2}\,(\mu L) \tag{18}$$

The pressure drop across the outlet distributor with a changing hydraulic diameter can be estimated by simplifying the Darcy-Weisbach equation and integrating the hydraulic diameter over the length of the outlet distributor. After plugging in for the friction factor and Reynolds number, this equation simplifies to

$$\Delta P_{dist-out} = \frac{32{*}\mu{*}l_{dist-out}{*}Q_{ch}}{\int_0^{l_{dist-out}} \left(A{*}D_H^2\right)dx}\,(\text{Pa}) \tag{19}$$

The total pressure drop across the chambers is the sum of the pressure drop across the chambers, inlet distributor, and outlet distributor:

$$\Delta P_{ch} = \Delta P_{ch} + \Delta P_{dist-in} + \Delta P_{dist-out} \tag{20}$$

Finally, the pressure drop through the channels or piping has to be determined. The piping dimensions and flow rates were first defined:

$$\text{Width of piping} = w_p = w_{dist-out} = w_{dist-in}\,(\mu\text{m})$$

$$\text{Length of piping} = l_p\,(\mu\text{m})$$

$$\text{Height of piping} = h_p\,(\mu\text{m})$$

$$\text{Number of fluidic streams or pathways} = N_{streams}$$

$$\text{Number of bends } \left(90^{\circ} \text{ turns}\right) \text{ in the pathways} = N_{bends}$$

$$\text{Flow rate in piping} = \text{flow rate in chambers} = Q_p = Q_{ch}\,(\mu\text{L}/\text{min})$$

$$\text{Piping average velocity} = u_p = \frac{Q_p}{w_p{*}h_p}\,(\mu\text{m}/\text{min}) \tag{21}$$

$$\text{Piping hydraulic diameter} = D_{Hp} = \frac{2{*}w_p{*}h_p}{w_p + h_p}\,(\mu\text{m}) \tag{22}$$

$$\text{Piping Reynolds number} = \frac{\rho * u_p * D_{Hp}}{\mu} \tag{23}$$

Pressure drop in the channels or piping can be calculated using the Darcy-Weisbach equation (Eq. 12) with the piping average velocity, length, and hydraulic diameter:

$$\Delta P_p = \frac{f * \rho * l_p * u_p^2}{2 * D_{Hp}} \text{ (Pa)} \tag{24}$$

Finally, the minor losses or pressure drop due to pipe fittings was calculated. K, the loss coefficient, is needed for these calculations. K values depend on the pipe diameter and the Reynolds number and, in this example, were set to 0.7 for the 90° square elbow bends in the channels connecting the inlet, chambers, and outlet [22]. The pressure drop due to fittings was calculated using [22] the following:

$$\Delta P_f = \frac{K * u_p^2 * \rho}{2} * N_{bends} \text{ (Pa)} \tag{25}$$

The total pressure drop for each fluidic stream was then determined simultaneously by adding the pressure drop through the chambers, piping, and fittings because they are in series:

$$\Delta P_{Stream} = \Delta P_{ch} + \Delta P_p + \Delta P_f \text{ (Pa)} \tag{26}$$

The pressure drop for fluidic streams should be balanced. Ideally, the value for each stream should be within 5% or less of the others. Note that in this example, the pressure drop across the fat compartment is calculated like that of a channel, because the fat chamber is simply a long channel. The pressure drop is very sensitive to the width of the piping, which can be adjusted to equalize pressure drop for each stream during the chip design. When the device is fabricated and operated, the pressure drops will be even, and the flow rates will adjust accordingly. Therefore, if the pressure drop calculations are inaccurate, the flow rate and residence time in each chamber will not match the desired values. Experimental measurements of flow rate through each chamber can be performed with fluorescent beads or by tracking oil/water interface movement through piping and chambers as described previously [14,23–25]. Other important parameters that can be calculated once the flow rates, chamber sizes, and piping dimensions are determined include total volume on the chip, total residence time on the chip, and total pressure drop, which is calculated by summing the inverse of each parallel stream:

$$\text{Total chip volume} = V_{Chip} = w_p * h_p * l_p + w_{ch} * h_{ch} * l_{ch} + V_{dist-in} + V_{dist-out} \text{ (μL)} \tag{27}$$

$$\text{Total chip residence time} = \frac{V_{Chip}}{Q_{Total}} \text{ (s)} \tag{28}$$

$$\text{Total chip pressure drop} = \Delta P_{Total} = \sum_{i=0}^{N_{streams}-1} \frac{1}{\frac{1}{\Delta P_{streams_i}}} \text{ (Pa)} \tag{29}$$

2.3 FABRICATING TISSUE-ON-A-CHIP AND BODY-ON-A-CHIP DEVICES

One of the first systems of interconnected tissue compartments that was developed to test the concept of a multiorgan system was realized in 1995. The system was constructed with standard-sized glass dilution bottles and commercially available tubing [26,27]. The bottles were filled with liver tissue and lung tissue from rats, and cell culture medium was recirculated between them and another bottle that represented the liquid portion of all other organs that were not represented by a cell culture. The device was used to investigate whether naphthalene, a known toxicant, was metabolized in the liver and whether the resulting metabolite was toxic to lung tissue. That proof-of-concept system worked as intended and replicated lung toxicity as a result of naphthalene exposure. But the standard sizes of bottles and tubing made it difficult to replicate physiological relationships of organ sizes and physiological fluidic flow.

Today, body-on-a-chip developers use 3-D printing or microfabrication to construct their devices. Both methods offer distinct advantages, leading to more physiologically correct mimics of the human body. First, chamber and channel sizes can be custom designed so that they match physiological relationships better. Tissue chambers can also be fabricated to be relatively small, so high-quality tissues, as small as 10,000 cells, from expensive sources can be used. Second, channel sizes can be fabricated with high precision so that fluidic flow within them is much better controlled and physiological fluid flow patterns can even be achieved with passive flow controls.

Microfabrication can also be used to create three-dimensional microscaffolds for constructing tissues with more physiological microarchitecture. For example, the 3-D structure of the microvilli of the GI tract and the niche-dependent growth of bacteria on them have been recreated [28–32]. Using poly(dimethylsiloxane) (PDMS) membranes, researchers have also microfabricated devices that were capable of growing lung tissue under the mechanical forces that are so characteristic of lung tissue in vivo [33,34].

The precise dimensions of microfluidic interconnects enable the design of system passive fluidic controls. Fluidic flow can be controlled passively through balancing pressure drops at flow splits and through building channels with varying hydraulic resistances. Passive flow control allows devices to be operated with gravity to drive fluidic flow and to eliminate the need for peristaltic pumps or syringe pumps. This in turn eliminates the need for tubing. Body-on-a-chip systems often operate with an excess of liquid in order to fill the tubing, and the ability to work without tubing allows for a decrease in liquid amount needed and with that a more physiological liquid-to-cell ratio.

Because microfabrication techniques were originally developed for the construction of transistors on silicon substrates and later for the construction of microelectromechanical systems made from silicon, there are many microfabrication techniques available for silicon. In particular, the ability to etch silicon to a depth of 50 or 100 μm relatively fast (in about 25–50 min) led to the first microfabricated body-on-a-chip devices to be made in silicon [9,14,23–25,35]. Standard

photolithography techniques were used to define the chip pattern on a 500 μm-thick silicon wafer, and deep reactive ion etching was used to create the three-dimensional chamber and the channel network. The devices were closed with polycarbonate lids that were tightly screwed onto their top side, using a polycarbonate platform underneath. During the following years, fabrication methods that made use of other materials such as PDMS [33,36–38] and 3-D printed polymers [39] were developed. Both PDMS fabrication and 3-D printing are techniques that are inexpensive and allow for rapid prototyping. Three-dimensional printing also allows for building complex 3-D structures that might not be possible with other fabrication techniques.

When choosing a microfabrication technique for the construction of body-on-a-chip systems (and with that the material the devices will consist of), it is important to consider the impact the building material has on the performance of the device. Silicon devices are biocompatible but need to be coated with extracellular matrix in order to retain cells within the tissue chambers. Devices made from PDMS are also biocompatible but have the disadvantages that they can only be used with a limited number of drugs. The material is known to adsorb hydrophobic drugs and metabolites, making toxicity data obtained with those devices unreliable. A similar concern exists for silicone tubing [40]. Because drug concentrations directly affect toxicity, devices are preferably made without silicone components. Materials that are used for 3-D printing can be incompatible with cell culture if they are not fully cured. Components can seep from the device's surface and into the cell culture medium. One way to remedy that problem is to coat the devices with a layer of parylene C. Parylene C can also significantly reduce drug and metabolite absorption into PDMS.

When constructing body-on-a-chip devices, it is important to consider the material they are made of. It is becoming clear that easy to work with materials like PDMS and silicone gaskets can absorb hydrophobic drugs or metabolites. This is unfortunate, because such materials are excellent for sealing tissue chambers and prevent leaking. However, to obtain accurate results, it is important to consider drug-material interactions and avoid unnecessary complications.

When barrier tissues such as the lung, GI tract epithelium, or kidney epithelium are part of the body-on-a-chip device, the device must also contain a porous membrane so that drug transport across those tissues can take place. This membrane must be accessible from both sides. A large selection of membranes made from polymers is available commercially. There are also some microfabricated membranes that can be used such as SU-8 membranes [29], silicon nitride membranes [41], and stretchable PDMS membranes [42]. Those membranes have the advantage of being transparent, having a high porosity, and being ultrathin.

2.4 MEASURING TISSUE RESPONSES WITHIN BODY-ON-A-CHIP PLATFORMS

On-chip integrated sensors are key to making body-on-a-chip platforms useful beyond proof-of-concept experiments. Ultimately, the responses of tissues to drugs need to be measured over a period of several hours, days, or even weeks. Early devices

have simply measured cell survival after a drug exposure. Medium samples taken from the devices can also provide data about the rate of metabolism of cells. For example, liver tissue metabolism can be assessed by collecting medium samples and determining the albumin and urea content in them. Liver tissue enzymes (such as CYP450 enzymes) can also be probed for their activity by supplying substrates and measuring the amount of converted substrate in the cell culture medium recovered from the system. But to obtain more detailed information, sensors that measure how well the cells are functioning over the course of a drug exposure are needed.

On-chip sensors can be categorized as electric, optical, and mechanical. Optical imaging tools, such as fluorescent dyes, exist for a large number of applications and can be utilized with body-on-a-chip systems as well [43]. If the system has a glass cover or a nonautofluorescent plastic cover such as one made from polystyrene, then fluorescent dyes can be used to image the tissues within. Integrated optical waveguides can eliminate the need for the use of a microscope and will ultimately allow for the building of more advanced systems [44]. Ultrasensitive CMOS cameras can detect even single molecules, but have not yet been integrated into complex body-on-a-chip systems [45].

Electric sensors are perhaps the easiest to integrate into body-on-a-chip systems. They can be fabricated on an insulating substrate, such as glass, or on top of an insulating layer of silicon nitride, silicon dioxide, or polymer. Their shape can be defined via lithography techniques, and metal layers are either evaporated or sputtered on top of the electrode pattern. Such electrodes typically consist of a thin metal layer (chrome or titanium, 2–5 nm thick) that promotes adhesion of a thicker gold or platinum layer that forms the actual electrode (150–200 nm). Microelectrode arrays (MEAs) consist of an assembly of such electrodes and have been used to record the electric properties of cardiomyocytes that were exposed to different conditions [46–48] and to assess neurotoxicity [49].

Another electrode system that can be integrated into body-on-a-chip devices are four electrode systems with two electrodes located on each side of a membrane. Those systems are capable of measuring the resistance across an endothelial or epithelial tissue layer [50]. This technique is often used to assess the interruption a drug causes to the barrier function of tissues such as the GI tract epithelium or the blood-brain barrier. Results from such custom-designed electrodes can, however, not be readily compared with those obtained with commercial systems since the electric field produced by the custom shapes (and distances) of the electrodes can be quite different from those of commercial electrodes. The placement of the electrode with regard to the barrier tissue through which the electric current passes influences the measured electric resistance. For that reason, any custom-made systems need to be calibrated in order to make the results obtained with them meaningful [50].

Mechanical sensors such as round oscillators and cantilevers can measure the mechanical properties of cells. Those sensors are most sensitive in an environment where their oscillation is not dampened by liquid (i.e., under vacuum), but recently, researchers have also used them to measure the contractile forces of live cells [51–53]. Another way to measure contractile forces is to use a pillar array made

of stretchable material [54] or growth surfaces that can be deformed by cells. In general, a wide variety of sensors exists, but few have been integrated with multiorgan body-on-a-chip platforms.

2.5 OPERATING BODY-ON-A-CHIP DEVICES

Body-on-a-chip devices have been operated anywhere from 24 h to several weeks. The operating time depends on the question that is asked. To determine whether a drug is acutely toxic, it might be sufficient to operate the device for a few hours. During short run times, it is possible that cells produce waste at a rate that does not interfere with the toxicity assay [25]. However, to determine whether a drug has chronic exposure effects on tissues, the exposure has to be conducted over several weeks [39], and a mechanism for waste removal has to be devised. The easiest method to remove cell waste is simply to replace part of the cell culture medium with fresh medium. Replacing significant amounts of medium within the system, however, will also affect drug and metabolite concentrations. That dilution effect must be taken into account when evaluating data obtained with the system.

The most challenging part of operating body-on-a-chip devices can be the placing of different tissues into the different cell culture chambers. A strategy that has worked well is to create temporary barriers on the open chip and seed the cells of different tissues into the chambers. After 24 h, all cells will be attached to the surface of the chip, and the chip can be closed with its cover. This strategy works well when working with cell lines and 2-D tissues.

A strategy that works better for highly specialized and for 3-D tissues is to create a modular device, where the tissues can grow in their own cell culture medium, separate from each other [39]. Once mature, the separate modules can be combined to build the larger system and to conduct toxicity experiments. Xu et al. have developed yet another approach, where cells are mixed with a UV-sensitive polymer that is pumped through the chip and only polymerized in the cell culture chamber that is appropriate for each cell type [55]. A strategy that requires more complex on-chip components would be to integrate separate channels and valves that lead up to each of the cell culture chambers and can be used to fill the chambers with cells.

A challenge related to placing tissues onto the platform is the formation of air bubbles and, after closing the devices, leaking of cell culture medium. Both air bubble formation and leaking would alter fluidic flow and drug exposure to each of the tissues and ultimately invalidate the experiment. While leaking can be prevented by engineering a well-thought-out closing mechanism for the devices, the formation of air bubbles is not easy to prevent. To keep air bubbles from traveling throughout the system and damaging tissues, Sung et al. have developed a bubble trap that captures air bubbles [56]. We have also found that operating devices with gravity-driven flow reduce the risk of leaking and air bubble formation. Several devices have been developed for use with gravity [39,52,57].

3 MIMICKING THE METABOLISM OF THE HUMAN BODY: EXAMPLES OF PROOF-OF-CONCEPT STUDIES

3.1 DEVELOPMENT OF CELL CULTURE ANALOGS (CCAs)

As mentioned in Section 2.3, the first three-component cell culture analog (CCA) was developed in 1995 by Sweeney et al. to study the toxicology of naphthalene [26]. The concept of a CCA was to combine several bioreactors containing different mammalian cell cultures to represent the organs and tissues in an animal. Recirculating culture medium pumped through the bioreactors represented the circulatory system, and all bioreactor dimensions and corresponding culture medium flow rates were scaled down from the actual organ or tissue sizes and blood flows in vivo. The resulting system was a replicate of the corresponding (PBPK) model of the animal with the ability to experimentally study the dynamics of dose exposure, including metabolite exchange between tissues. The ability to experimentally study the dosing conditions of compounds and the inclusion of metabolite exchange between tissues is an advantage over standard in vitro culture techniques. Unlike standard, single-cell-type, 2-D in vitro systems, a CCA can mimic the dynamics of dose exposure. Because any cell type may be used, the CCA devices can be designed to mimic key target organs from mice, rats, dogs, or humans, by selecting representative cell lines and designing corresponding culture vessels.

The first CCA system was constructed using milk dilution bottles as culture vessels, with tubing connecting each bottle and peristaltic pump providing recirculating flow [26]. The CCA was used to mimic rat naphthalene exposure. Naphthalene is only moderately toxic in its native form but can induce lung tissue damage after becoming activated by metabolism in the liver. The initial CCA contained a liver and lung compartment modeled by monolayers of H4IIE, a rat liver hepatoma cell line, and L2, a rat lung cell line. A bottle without cells modeled the remainder of the rat's organs and tissues and acted as a nonmetabolizing body of distribution. No cells were needed in the "other tissue" compartment because the liver and lung are the organs most affected by naphthalene and its metabolites. The H4IIE cells have cytochrome P4501A1 (CYP1A1), epoxide hydrolase, and glutathione-S-transferase activity, which are needed for the metabolism of naphthalene to the epoxide form, conversion to dihydrodiol, and conjugation with glutathione, respectively. L2 cells do not express the enzymes needed for naphthalene activation.

Experiments with this first CCA [26] showed that naphthalene induced lung cell toxicity (lactate dehydrogenase or LDH release and glutathione or GSH depletion) after naphthalene was metabolized by liver cells and reactive metabolites circulated to the lung compartment. Increasing CYP1A1 activity by increasing the number of liver cells or increasing CYP1A1 activity also increased the toxicity to the lung cells. In experiments with no liver cells present, there was no toxicity observed in the lung cells. There were several drawbacks to this system, however, including nonphysiological fluid-to-tissue ratios and organ residence times and a design that was complicated to operate and did not allow for straightforward time-course studies.

A revised CCA was constructed by Ghanem and Shuler to address some of the concerns with the prototype CCA [27]. The modified system used a packed-bed design, where H4IIE and L2 rat cells were cultured on microcarrier beads within the milk dilution bottles. The addition of microcarrier beads increased the fluid-to-tissue ratio and allowed for time-course sampling of cells during experiments via periodic bead removal with a sterile syringe. Liquid residence times within the organ compartments were improved in this system but were still longer than physiological residence times due to the limited flow through the packed beds. Unlike the prototype system, no response to naphthalene was observed. In the prototype system by Sweeney et al. [26], a long liquid residence times in the liver compartment allowed for the formation of a relatively large amount of toxic naphthalene metabolites, while in the packed-bed system, shorter liver liquid residence times resulted in negligible toxic metabolite formation. This difference in naphthalene response between the initial monolayer CCA and packed-bed CCA designs was explained with PBPK models of each CCA [58], demonstrating how a PBPK model can provide a mechanistic basis for understanding differences in CCA response due to different experimental configurations.

The CCA concept was revised with the design of a three-compartment (liver-lung-other tissue) micro cell culture analog (μCCA) [14]. The μCCA was microfabricated from silicon with tools from the semiconductor industry. The μCCA devices allow for near in vivo residence times and fluid-to-tissue volume ratios, are relatively high throughput and inexpensive to fabricate, have a low volume that conserves reagents and cells, and facilitate automated collection and processing of data. The first μCCA device used the same H4IIE and L2 cell lines of the previous CCA systems, but the chip was 2.5 × 2.5 cm in dimension and enclosed by a plastic housing. Cells were attached to the culture chambers with a combination of poly-D-lysine and Matrigel (for H4IIE) or fibronectin (for L2). Additionally, an integrated oxygen sensor was incorporated into the chip. This sensor used a ruthenium dye immobilized in a resin as a UV-sensitive indicator of dissolved oxygen content, which demonstrates the potential to build real-time sensors into a device.

Building on the first μCCA design, a second μCCA was designed that was similar to the first design but divided the other tissue compartment into well-perfused and slowly perfused chambers or lung-liver-other tissues-fat compartments [23]. The liver cell line H4IIE was replaced with a human hepatoma line HepG2/C3A due to increased CYP activity. Naphthalene was again used to test the system and was shown to cause a significant decrease in lung and liver cell GSH after 6 h of exposure. When no liver cells were present, there was no GSH depletion in the lung cells, again indicating that naphthalene biotransformation by the liver cells produces a metabolite that is toxic to the lung cells. Further experiments in this μCCA identified the reactive metabolites to be 1,2-naphthalenediol and 1,2-naphthoquinone. This discovery showed the utility of the μCCA system in investigating toxicity mechanisms.

To further elucidate naphthalene toxicity, Viravaidya and Shuler used a μCCA to investigate the role of bioaccumulation or the storage of compounds within fat tissue on the response of the μCCA system to naphthalene compounds [59]. The rat

preadipocyte cell line 3T3-L1 was used to model fat within the fat chamber due to the ability to attach this cell line to the silicon surface. Experiments with naphthalene and 1,2-naphthoquinone showed that sequestering of naphtha compounds by the fat cells reduced GSH depletion in both liver and lung cells when compared with a system with no fat cells. This illustrates the utility of this μCCA system to explore the impact of dosing dynamics on toxicity.

3.2 μCCA-BASED BODY-ON-A-CHIP SYSTEMS FOR TOXICITY TESTING

Later studies with multicell-type, microfabricated μCCAs further demonstrated the value of μCCA devices coupled with PBPK models for drug testing. Sung and Shuler [25] used a 3-D μCCA device with liver and colon cells encapsulated in Matrigel to determine the cytotoxic effects of Tegafur. Tegafur is a cancer drug that is metabolized by the liver to 5-fluorouracil (5-FU), which acts as a chemotherapeutic agent for colon cancer. In μCCA devices without liver cells, Tegafur was ineffective against colon cancer cells (HCT-116). When HepG2/C3A liver cells were added to the liver compartment, Tegafur was converted to 5-FU by CYP450 enzymes, and the 5-FU had significant toxic effects on HCT-116 colon cancer cells. Tegafur activity against HCT-116 colon cancer cells was not observed in well plate experiments with only colon cancer cells, and the results observed in this μCCA study were only previously seen in animal experiments or clinical studies involving humans.

Another μCCA system developed by Sung and Shuler contained liver cells, colon cancer cells, and myeloblasts that were subjected to 5-fluorouracil (5-FU, an anticancer drug) plus uracil [35]. Experiments with the μCCA device used concentrations similar to human clinical doses. Uracil is a natural substrate for the enzyme that metabolizes 5-FU, and uracil is often administered clinically in combination with 5-FU to improve 5-FU effects [60]. In this study, the PBPK model predicted a differential cell response to 5-FU, with liver cells that were more resistant and myeloblasts more sensitive, and the μCCA experiments demonstrated that a combination of 5-FU and uracil enhanced cytotoxic effects compared with 5-FU alone. These results are consistent with human response to the drugs.

Tatosian and Shuler [24] showed that μCCAs could be used to study the synergistic effects of cancer drugs and to test whether a combination of drugs could replace a single drug that is known to have strong side effects. The μCCA device used for this study was designed to include two uterine cancer compartments with the cell line MES-SA and its multidrug resistant (MDR) variant MES-SA/DX-5, a liver compartment that contained HepG2/C3A for drug metabolism, a bone marrow compartment containing the megakaryoblast cell line MEG-01 to represent a tissue highly susceptible to the effects of chemotherapy, and other tissue compartment. Experiments were conducted with the chemotherapeutic doxorubicin and two multidrug resistance (MDR) suppressors, cyclosporine and nicardipine. When the μCCA was "treated" with doxorubicin and either cyclosporine or nicardipine, the proliferation of the MDR uterine cancer cells was reduced when compared with

doxorubicin-only treatment. More importantly, a combination of nicardipine and cyclosporine decreased MDR cell growth rate more effectively than a higher concentration of either MDR modulator alone. This synergistic interaction between the two modulators was not observed in multiwell plate assays.

Mahler et al. developed a μCCA system that was capable of mimicking the oral uptake and first-pass metabolism of drugs and drug carriers in humans [9]. First-pass metabolism occurs when drug is absorbed by the GI tract and passes via the portal vein to the liver where the drug is metabolized. A result of first-pass metabolism is that the concentration of a drug is greatly reduced before it reaches systemic circulation. The results of first-pass metabolism include low drug bioavailability in the systemic circulation and potentially toxic effects on the liver and GI tract tissues. The μCCA was designed with three compartments (GI-liver-other tissues) with a Caco-2/HT29-MTX coculture representing the intestine and HepG2/C3A representing the liver. This system successfully simulated the absorption and metabolism of acetaminophen. Both epithelial cells and liver cells metabolized acetaminophen to toxic metabolites via CYP450 enzymes, resulting in a dose-dependent decrease in liver cell viability that correlated well with previously published acetaminophen liver injury studies in mice.

The same GI-liver-other tissues μCCA was used to simulate the oral uptake of 50 nm carboxylated polystyrene nanoparticles [13]. The use of nanoparticles in medical applications is highly anticipated, but little is known about how they will affect human tissues. Polystyrene nanoparticles were administered at physiologically realistic doses, and the transport of nanoparticles across the Caco-2/HT29-MTX coculture, which mimics nanoparticle ingestion, showed that most nanoparticles that reached the systemic circulation were single nanoparticles and small aggregates. After crossing the GI tract epithelium, nanoparticles induced the release of aspartate aminotransferase (AST), a liver enzyme that indicates liver cell injury. Using the GI tract-liver-other tissue allowed for the observation of compounding effects and the detection of liver tissue injury at lower nanoparticle concentrations than expected from experiments with liver tissue only. These results show that body-on-a-chip devices are highly relevant in vitro models for evaluating nanoscale particle and drug-carrier interactions with human tissues.

Most body-on-a-chip systems require an external pump to drive fluid flow through the device. The pump adds additional cost, limits the number of devices that can be run at one time, complicates operation, requires polymeric tubing that can adsorb materials, can result in bubble formation or entrapment, and generally provides shear stress rates that are higher than those experienced by organs and tissues in the body, that is, <0.2 N/m^2 (2 dyn/cm^2) [35,57]. Sung et al. [35] first developed a multilayer, 3-D μCCA design, which housed cells cultured within hydrogels and operated with pumpless gravity-induced flow to test the toxicity of the anticancer drug, 5-FU. Each cell type mimicking a tissue (liver-tumor tissue-marrow) exhibited differential responses to 5-FU, the cellular responses in the microfluidic environment were different from those in the static environment, and the response was similar to what was anticipated from animal studies.

Miller and Shuler [57] next developed a pumpless, 14 compartment body-on-a-chip system. The design is for 13 organs using 14 chambers, with 2 chambers used for the skin. A barrier layer containing skin, GI, and lung epithelial cells is directly exposed to compounds of interest, and the barrier tissue layer separates chambers containing nonbarrier tissue cultures seeded into 3-D hydrogels, including the fat, kidney, heart, adrenal glands, liver, spleen, pancreas, bone marrow, brain, and muscle. Gravity was used to drive physiologically realistic flow through the channels by placing the device on a rocker platform. Preliminary experiments with the device showed that five different cell lines had high viability and retained cell type-specific function for 7 days in the fluidic device.

Finally, Oleaga et al. have developed a four-organ body-on-a-chip system with pumpless recirculation of a serum-free medium to test the response of the human cardiac, liver, skeletal muscle, and neuronal cultures to five different drugs for at least 14 days [52]. These cell types were chosen to provide insight into important metabolic and functional changes in human tissues in response to challenge with compounds with well-defined toxicological properties. The compounds studied were doxorubicin, a chemotherapy drug; atorvastatin, a cholesterol lowering medication; valproic acid, a treatment for epilepsy and bipolar disorder; acetaminophen, a pain reliever and fever reducer; and a control compound, *N*-acetyl-m-aminophenol, which is a nontoxic isomer of acetaminophen. The toxicity trials were initiated after 5 days of culture under flow in the pumpless system and lasted for 48 h. Comparison of results within the multiorgan device with human clinical data or other data from the literature shows agreement between the in vitro platform and clinical observations on humans. This provides initial validation of the microphysiological system as a model for accurately predicting multiorgan toxicity in humans and indicates that the in vitro system is a viable tool to study organ-to-organ communication, drug toxicity, drug-drug interactions, and novel drug compound effects in humans for predictive purposes in acute or chronic studies.

3.3 OTHER MULTIORGAN CULTURE SYSTEMS

Development of body-on-a-chip systems is a very active area of research, and a number of recent reviews have summarized progress in the area [7,61,62]. Several proof-of-concept studies have shown that metabolites formed in one organ compartment can indeed travel to other organ compartments and affect the tissues there. In 2013, Choucha-Snouber et al. published their results from a study that included two organs (the liver and kidney) within one microfluidic body-on-a-chip system [37]. They exposed the system to a cancer prodrug (ifosfamide) to see if the nephrotoxic metabolite formed in the liver will affect the kidney tissue in the kidney compartment. Without liver cells, no toxicity was observed, but when HepaRG liver cells were present in the system, the number of kidney cells was reduced because of toxicity. This effect was not seen, however, with HepG2/C3A liver cells, and one of the conclusions of the study was that HepG2/C3A liver cells lack the capacity for transforming ifosfamide into a nephrotoxic metabolite.

In 2017, Bauer et al. published a device that contained liver spheroids in one tissue compartment and pancreatic islets in another [63]. When glucose was added to

the system that was operated with insulin-free medium, the pancreatic islets produced insulin, which in turn increased glucose consumption in the liver. As the glucose concentration fell as a result of consumption in the liver, the insulin production in the islets decreased as well. This feedback loop between the tissues mimics their function inside the human body and can be used to study diseases like type 2 diabetes.

Two recent studies have tackled the challenge of including more organ compartments into a single body-on-a-chip system [52]. Maschmeyer et al. have developed a four-organ chip that combined skin, intestine, liver, and kidney tissues [64]. The device was operated for 28 days with cellular waste being removed through the kidney tissue. Similarly, Oleaga et al. have developed a system with the liver, cardiac cell, muscle cells, and neurons and operated it in a pumpless device for 14 days [52]. Both studies proved that multiple tissues can function well within one system using a common cell culture medium.

4 WHAT IS THE FUTURE OF BODY-ON-A-CHIP SYSTEMS?

4.1 POTENTIAL

Body-on-a-chip devices have the potential to aid in the drug discovery process in many ways. If designed with human physiology in mind, the devices will mimic drug human metabolism when challenged with a drug. Results obtained with the devices may even predict what will happen in the human body better than current animal models. The devices also offer experimental capabilities that cannot be achieved with animal models. For example, a device could be operated without a particular organ to see how that organ influences the metabolism of a drug. An organ could also be made bigger on the device than it is in the human body to probe how the drug metabolism changes. Results obtained with such unnatural systems could give us information about what the pathway of a drug is and where toxic metabolites originate.

The devices are also very well suited to be used with tissues that represent a particular population. It could be used with breast tissue with and without mutation in the BRCA genes to see how different those two populations would respond to a drug. One can also imagine that devices are constructed for men, women, or children of different ages. This would lead to a path out of the bias created by using mostly male animals in preclinical trials [65]. Devices could also be operated with biopsy samples from a particular patient or a patient's tissues derived from iPS cells. Vunjak-Novakovic et al. have demonstrated a two-organ device (liver and cardiac tissues) with associated microvascular cells that has accomplished this [66]. Devices like that can lead the path into personalized medicine.

4.2 NEEDS

In order to realize that potential, however, many unaddressed issues need to be resolved. First, body-on-a-chip platforms need to be designed to mimic human physiology rather accurately. There are several tools available for developing platform design criteria. Simplified PBPK models can guide the design as described above, and the devices can be tested for the mathematically predicted outcome.

A thorough validation of design criteria could begin with the development of simplified PBPK models for animals, the building and testing of the related animal-on-a-chip devices, and the appropriate animal experiments. Comparing the results from all three approaches will give us information about how well the animal-on-a-chip device performed and how data from such devices could be used to develop devices that mimic the human body well.

While organ size ratios and human fluid residence times have been achieved, the more difficult issue of reaching a physiological liquid-to-cell ratio is still a challenge. Currently, body-on-a-chip devices contain liquid-to-cell ratios that are from 10- to 100-fold the physiological value. Too much liquid within the devices will dilute drug and metabolites and skew toxicity measurements. On the other hand, too little liquid would challenge the cell survival and the availability of enough liquid for measurements and analyses.

Tissues in vivo are three-dimensional, and 3-D cell culture can improve the cell differentiation and/or function when compared with 2-D culture [29]. Natural and synthetic hydrogels have been used in body- and organ-on-a-chip models. Three-dimensional cell culture within microfluidic devices has been achieved with natural hydrogels including collagen, gelatin, alginate, and agarose, while synthetic hydrogels used in microfluidics include polyethylene gly*co*l and poly(lactic-co-glycolic acid) [7]. A 3-D cell culture not only can more closely mimic the in vivo environment by recreating cell-cell and cell-extracellular matrix interactions but also may result in unwanted adsorption or limited nutrient, oxygen, or waste transfer.

Further, in order to mimic the human body well, primary cells and stem-cell-derived cells should be used to construct the tissues that are placed into the device. Such cells would mimic human tissues better than would immortalized cell lines. However, a challenge that arises from the use of those cells is to find a common cell culture medium that satisfies the requirements of all the cells present in the system.

4.3 IN VITRO TO IN VIVO EXTRAPOLATION (IVIVE)

Data obtained with body-on-a-chip devices can be extrapolated to the human body, to predict drug efficacy and toxicity in humans. The closer the system mimics the conditions inside the human body, the more authentic will be the metabolic system created within, and the easier it becomes to make predictions based on the data obtained with the system. Ideally, if the conditions are exactly like they are inside the body, then metabolite concentrations within the system would be the same as in vivo. However, that is difficult to achieve, and mathematical adjustments will need to be made in the human PBPK model that is used to predict the outcome for patients. The following conditions need to be accounted for:

(1) The cell density inside the body is much higher than it is in most in vitro tissues, and as a result, it is difficult to replicate physiological liquid-to-cell ratios inside body-on-a-chip devices. The human body contains about 4–6 L of blood [67]. If organ compartments represent tissue slices that are 1/100,000 of the

corresponding organ in the human body, then the amount of blood surrogate within the system should be between 40 and 60 μL. In addition to blood, the body contains interstitial fluid. Partitioning of compounds from blood into that fluid can be rapid and can dilute drugs and drug metabolites. Such interstitial fluid volumes also need to be added to body-on-chip devices. When developing body-on-a-chip systems, care must be taken to design them so that the liquid-to-cell ratio is physiological. If that is not the case, toxicity in the device might be skewed toward less toxic observations than what should be the case in patients. That needs to be taken into account when evaluating data from body-on-a-chip devices.

(2) Cells do not function at the same level outside the body as they do inside, because many of the biochemical and biophysical cues that play a role in their functioning are lost when the cells are harvested. Enzyme activities decline as soon as the cells are removed from the body. Cocultures with multiple cell types can alleviate the decline in functionality. However, cells are not likely to reach the exact same level of performance as inside the body.

Devices that achieve high cell density with 3-D tissues and low liquid-to-cell ratios and that utilize primary cells or stem-cell-derived tissues will give results that will predict best what will happen in the human body.

4.4 COMMERCIALIZATION

The devices not only need to work well but also need to be adopted by drug developers. That would be easiest if the devices are inexpensive, easy to operate, and reliable. The aforementioned problems with leaking of cell culture medium and air bubble formation need to be solved in order to make the devices more reliable. Recently, pumpless systems that are suitable for massive parallelization have been demonstrated [35,39,52,57]. Some of the systems move the cell culture medium back and forth through the device, and others have built-in mechanisms that recirculate the medium in one direction. This becomes particularly important once the systems contain endothelial cells that are sensitive to the direction of shear [39]. Simple, pumpless single-organ systems have already been commercialized [68–70]. The commercialization of organ-on-a-chip platforms has been summarized by Zhang and Radisic [71]. Criteria could include the system's liquid-to-cell ratio and liquid residence times within a defined tissue volume, tissue sources, or enzyme activity.

5 CONCLUSIONS

Collecting accurate efficacy and toxicity data on compounds early enough to direct resources to the best drug candidates has both economic and ethical value. Body-on-a-chip devices, particularly when used in conjunction with the corresponding PBPK, offer the possibility of making more realistic models that can act as surrogates for

animals and humans in toxicity testing. Although there are still significant challenges that remain in the field, continued research into body-on-a-chip development, characterization, and validation has the potential for providing breakthroughs in drug discovery, disease modeling, and our fundamental understanding of organ and tissue interactions.

DISCLAIMER

Commercial equipment, instruments, or materials are identified in this paper in order to specify the experimental procedure adequately. Such identification is not intended to imply recommendation or endorsement by the National Institute of Standards and Technology nor is it intended to imply that the materials or equipment identified is necessarily the best available for the purpose.

REFERENCES

[1] DiMasi JA, Grabowski HG, Hansen RW. Innovation in the pharmaceutical industry: new estimates of R&D costs. J Health Econ 2016;47:20–33. Epub 2016/03/02, https://doi.org/10.1016/j.jhealeco.2016.01.01226928437.

[2] CMR International. Pharmaceutical R&D executive summary. Thomson Reuters; 2015. Available from: http://cmr.thomsonreuters.com/pdf/Executive_Summary_Final.pdf. Accessed 15 December 2017.

[3] Martignoni M, Groothuis GMM, de Kanter R. Species differences between mouse, rat, dog, monkey and human CYP-mediated drug metabolism, inhibition and induction. Expert Opin Drug Metab Toxicol 2006;2(6):875–94. https://doi.org/10.1517/17425255.2.6.875.

[4] Shanks N, Greek R, Greek J. Are animal models predictive for humans? Philos Ethics Humanit Med 2009;4(1):1–20. https://doi.org/10.1186/1747-5341-4-2.

[5] Greek R, Menache A. Systematic reviews of animal models: methodology versus epistemology. Int J Med Sci 2013;10(3):206–21. https://doi.org/10.7150/ijms.5529. PMC3558708.

[6] Bhatia SN, Ingber DE. Microfluidic organs-on-chips. Nat Biotechnol 2014;32(8):760–72. Epub 2014/08/06, https://doi.org/10.1038/nbt.298925093883.

[7] Lee SH, Sung JH. Organ-on-a-chip technology for reproducing multiorgan physiology. Adv Healthc Mater 2017. Epub 2017/09/26, https://doi.org/10.1002/adhm.201700419289450001.

[8] Abaci HE, Shuler ML. Human-on-a-chip design strategies and principles for physiologically based pharmacokinetics/pharmacodynamics modeling. Integr Biol 2015;7(4):383–91. https://doi.org/10.1039/c4ib00292j.

[9] Mahler GJ, Esch MB, Glahn RP, Shuler ML. Characterization of a gastrointestinal tract microscale cell culture analog used to predict drug toxicity. Biotechnol Bioeng 2009;104(1):193–205. Epub 2009/05/07, https://doi.org/10.1002/bit.22366194185 62.

[10] Leclerc E, Hamon J, Bois FY. Investigation of ifosfamide and chloroacetaldehyde renal toxicity through integration of in vitro liver-kidney microfluidic data and pharmacokinetic-system biology models. J Appl Toxicol 2016;36(2):330–9. Epub 2015/07/15, https://doi.org/10.1002/jat.319126152902.

[11] Bhise NS, Ribas J, Manoharan V, Zhang YS, Polini A, Massa S, et al. Organ-on-a-chip platforms for studying drug delivery systems. J Control Release 2014;190:82–93. Epub 2014/05/14, https://doi.org/10.1016/j.jconrel.2014.05.00424818770.
[12] Stone HA. In: Hakho L, Westervelt RM, Ham D, editors. CMOS Biotechnology. New York: Springer Science+Business Media, LLC; 2007.
[13] Esch MB, Mahler GJ, Stokol T, Shuler ML. Body-on-a-chip simulation with gastrointestinal tract and liver tissues suggests that ingested nanoparticles have the potential to cause liver injury. Lab Chip 2014;14(16):3081–92. Epub 2014/06/28, https://doi.org/10.1039/c4lc00371c24970651.
[14] Sin A, Chin KC, Jamil MF, Kostov Y, Rao G, Shuler ML. The design and fabrication of three-chamber microscale cell culture analog devices with integrated dissolved oxygen sensors. Biotechnol Prog 2004;20:338–45.
[15] Malek AM, Alper SL, Izumo S. Hemodynamic shear stress and its role in atherosclerosis. JAMA 1999;282(21):2035–42. Epub 1999/12/11, 10591386.
[16] Nerem RM, Alexander RW, Chappell DC, Medford RM, Varner SE, Taylor WR. The study of the influence of flow on vascular endothelial biology. Am J Med Sci 1998;316(3):169–75. Epub 1998/09/28, 9749558.
[17] Powers MJ, Domansky K, Kaazempur-Mofrad MR, Kalezi A, Capitano A, Upadhyaya A, et al. A microfabricated array bioreactor for perfused 3D liver culture. Biotechnol Bioeng 2002;78(3):257–69. Epub 2002/03/29, 11920442.
[18] Bird RB, Stewart WE, Lightfoot EN. Transport phenomena. New York: John Wiley and Sons, Inc.; 1960.
[19] Sung JH, Esch MB, Prot JM, Long CJ, Smith A, Hickman JJ, et al. Microfabricated mammalian organ systems and their integration into models of whole animals and humans. Lab Chip 2013;13(7):1201–12. Epub 2013/02/08, https://doi.org/10.1039/c3lc41017j23388858.
[20] Munson BR, Young DF, Okiishi TH. Fundamentals of fluid mechanics. 3rd ed. New York: John Wiley and Sons, Inc.; 1998.
[21] Treybal RE. Mass-transfer operations. 3rd ed. New York: McGraw-Hill; 1982.
[22] Welty J, Wicks CE, Rorrer GL, Wilson RE. Fundamentals of momentum, heat, and mass transfer. 5th ed. New York: John Wiley & Sons, Inc.; 2007.
[23] Viravaidya K, Sin A, Shuler ML. Development of a microscale cell culture analog to probe naphthalene toxicity. Biotechnol Prog 2004;20(1):316–23.
[24] Tatosian DA, Shuler ML. A novel system for evaluation of drug mixtures for potential efficacy in treating multidrug resistant cancers. Biotechnol Bioeng 2009;103(1):187–98. https://doi.org/10.1002/bit.22219.
[25] Sung JH, Shuler ML. A micro cell culture analog (microCCA) with 3-D hydrogel culture of multiple cell lines to assess metabolism-dependent cytotoxicity of anticancer drugs. Lab Chip 2009;9(10):1385–94. Epub 2009/05/07, https://doi.org/10.1039/b901377f19417905.
[26] Sweeney LM, Shuler ML, Babish JG, Ghanem A. A cell culture analogue of rodent physiology: application to naphthalene toxicology. Toxicol In Vitro 1995;9(3):307–16. Epub 1995/06/01, 20650092.
[27] Ghanem A, Shuler ML. Characterization of a perfusion reactor utilizing mammalian cells on microcarrier beads. Biotechnol Prog 2000;16:471–9.
[28] Sung JH, Yu J, Luo D, Shuler ML, March JC. Microscale 3-D hydrogel scaffold for biomimetic gastrointestinal (GI) tract model. Lab Chip 2011;11(3):389–92. Epub 2010/12/16, https://doi.org/10.1039/c0lc00273a21157619.

[29] Esch MB, Sung JH, Yang J, Yu C, Yu J, March JC, et al. On chip porous polymer membranes for integration of gastrointestinal tract epithelium with microfluidic 'body-on-a-chip' devices. Biomed Microdevices 2012;14(5):895–906. Epub 2012/08/01, https://doi.org/10.1007/s10544-012-9669-022847474.

[30] Costello CM, Sorna RM, Goh YL, Cengic I, Jain NK, March JC. 3-D intestinal scaffolds for evaluating the therapeutic potential of probiotics. Mol Pharm 2014;11(7):2030–9. Epub 2014/05/07, https://doi.org/10.1021/mp500142224798584.

[31] Kim HJ, Ingber DE. Gut-on-a-chip microenvironment induces human intestinal cells to undergo villus differentiation. Integr Biol (Camb) 2013;5(9):1130–40. https://doi.org/10.1039/c3ib40126j. 23817533.

[32] Kim HJ, Li H, Collins JJ, Ingber DE. Contributions of microbiome and mechanical deformation to intestinal bacterial overgrowth and inflammation in a human gut-on-a-chip. Proc Natl Acad Sci 2016;113(1):E7–E15. https://doi.org/10.1073/pnas.1522193112. 26668389.

[33] Huh D, Matthews BD, Mammoto A, Montoya-Zavala M, Hsin HY, Ingber DE. Reconstituting organ-level lung functions on a chip. Science 2010;328(5986):1662–8. Epub 2010/06/26, https://doi.org/10.1126/science.118830220576885.

[34] Huh D, Fujioka H, Tung YC, Futai N, Paine 3rd R, Grotberg JB, et al. Acoustically detectable cellular-level lung injury induced by fluid mechanical stresses in microfluidic airway systems. Proc Natl Acad Sci U S A 2007;104(48):18886–91. Epub 2007/11/17, https://doi.org/10.1073/pnas.061086810418006663.

[35] Sung JH, Kam C, Shuler ML. A microfluidic device for a pharmacokinetic-pharmacodynamic (PK-PD) model on a chip. Lab Chip 2010;10(4):446–55. https://doi.org/10.1039/b917763a.

[36] Zhang C, Zhao Z, Abdul Rahim NA, van Noort D, Yu H. Towards a human-on-chip: culturing multiple cell types on a chip with compartmentalized microenvironments. Lab Chip 2009;9(22):3185–92. Epub 2009/10/30, https://doi.org/10.1039/b915147h 19865724.

[37] Choucha-Snouber L, Aninat C, Grsicom L, Madalinski G, Brochot C, Poleni PE, et al. Investigation of ifosfamide nephrotoxicity induced in a liver-kidney co-culture biochip. Biotechnol Bioeng 2013;110(2):597–608. Epub 2012/08/14, https://doi.org/10.1002/bit.2470722887128.

[38] Prot JM, Maciel L, Bricks T, Merlier F, Cotton J, Paullier P, et al. First pass intestinal and liver metabolism of paracetamol in a microfluidic platform coupled with a mathematical modeling as a means of evaluating ADME processes in humans. Biotechnol Bioeng 2014;111(10):2027–40. Epub 2014/06/24, https://doi.org/10.1002/bit.2523224954399.

[39] Esch MB, Ueno H, Applegate DR, Shuler ML. Modular, pumpless body-on-a-chip platform for the co-culture of GI tract epithelium and 3D primary liver tissue. Lab Chip 2016;16(14):2719–29. Epub 2016/06/23, https://doi.org/10.1039/c6lc00461j27332143.

[40] Xu H, Shuler ML. Quantification of chemical-polymer surface interactions in microfluidic cell culture devices. Biotechnol Prog 2009;25(2):543–51. Epub 2009/04/10, https://doi.org/10.1002/btpr.13519358211.

[41] Harris SG, Shuler ML. Growth of endothelial cells on microfabricated silicon nitride membranes for anin vitro model of the blood-brain barrier. Biotechnol Bioprocess Eng 2003;8(4):246–51. https://doi.org/10.1007/bf02942273.

[42] Huh D, Kim HJ, Fraser JP, Shea DE, Khan M, Bahinski A, et al. Microfabrication of human organs-on-chips. Nat Protoc 2013;8(11):2135–57. Epub 2013/10/12, https://doi.org/10.1038/nprot.2013.13724113786.

[43] Kuswandi B, Nuriman, Huskens J, Verboom W. Optical sensing systems for microfluidic devices: a review. Anal Chim Acta 2007;601(2):141–55. Epub 2007/10/09, https://doi.org/10.1016/j.aca.2007.08.04617920386.
[44] Jiang L, Gerhardt KP, Myer B, Zohar Y, Pau S. Evanescent-wave spectroscopy using an SU-8 waveguide for rapid quantitative detection of biomolecules. J Microelectromech Syst 2008;17:1495–500.
[45] Diekmann R, Till K, Muller M, Simonis M, Schuttpelz M, Huser T. Characterization of an industry-grade CMOS camera well suited for single molecule localization microscopy—high performance super-resolution at low cost. Sci Rep 2017;7(1):14425. Epub 2017/11/02, https://doi.org/10.1038/s41598-017-14762-629089524.
[46] Braam SR, Tertoolen L, van de Stolpe A, Meyer T, Passier R, Mummery CL. Prediction of drug-induced cardiotoxicity using human embryonic stem cell-derived cardiomyocytes. Stem Cell Res 2010;4(2):107–16. Epub 2009/12/26, https://doi.org/10.1016/j.scr.2009.11.00420034863.
[47] Meyer T, Boven KH, Gunther E, Fejtl M. Micro-electrode arrays in cardiac safety pharmacology: a novel tool to study QT interval prolongation. Drug Saf 2004;27(11):763–72. Epub 2004/09/08, 15350150.
[48] Natarajan A, Stancescu M, Dhir V, Armstrong C, Sommerhage F, Hickman JJ, et al. Patterned cardiomyocytes on microelectrode arrays as a functional, high information content drug screening platform. Biomaterials 2011;32(18):4267–74. Epub 2011/04/02, https://doi.org/10.1016/j.biomaterials.2010.12.02221453966.
[49] Hogberg HT, Sobanski T, Novellino A, Whelan M, Weiss DG, Bal-Price AK. Application of micro-electrode arrays (MEAs) as an emerging technology for developmental neurotoxicity: evaluation of domoic acid-induced effects in primary cultures of rat cortical neurons. Neurotoxicology 2011;32(1):158–68. Epub 2010/11/09, https://doi.org/10.1016/j.neuro.2010.10.00721056592.
[50] Srinivasan B, Kolli AR, Esch MB, Abaci HE, Shuler ML, Hickman JJ. TEER measurement techniques for in vitro barrier model systems. J Lab Autom 2015;20(2):107–26. Epub 2015/01/15, https://doi.org/10.1177/2211068214561025255869 98.
[51] Stancescu M, Molnar P, McAleer CW, McLamb W, Long CJ, Oleaga C, et al. A phenotypic in vitro model for the main determinants of human whole heart function. Biomaterials 2015;60:20–30. https://doi.org/10.1016/j.biomaterials.2015.04.035.
[52] Oleaga C, Bernabini C, Smith AST, Srinivasan B, Jackson M, McLamb W, et al. Multi-organ toxicity demonstration in a functional human in vitro system composed of four organs. Sci Rep 2016;6:20030. https://doi.org/10.1038/srep20030. http://www.nature.com/articles/srep20030#supplementary-information.
[53] Park J, Ryu J, Choi SK, Seo E, Cha JM, Ryu S, et al. Real-time measurement of the contractile forces of self-organized cardiomyocytes on hybrid biopolymer microcantilevers. Anal Chem 2005;77(20):6571–80. Epub 2005/10/15, https://doi.org/10.1021/ac050780016223242.
[54] Zhao Y, Zhang X. Cellular mechanics study in cardiac myocytes using PDMS pillars array. Sensors Actuators A Phys 2006;125(2):398–404. https://doi.org/10.1016/j.sna.2005.08.032.
[55] Xu H, Wu J, Chu CC, Shuler ML. Development of disposable PDMS micro cell culture analog devices with photopolymerizable hydrogel encapsulating living cells. Biomed Microdevices 2012;14(2):409–18. Epub 2011/12/14, https://doi.org/10.1007/s10544-011-9617-422160484.
[56] Sung JH, Shuler ML. Prevention of air bubble formation in a microfluidic perfusion cell culture system using a microscale bubble trap. Biomed Microdevices 2009;11(4):731–8. Epub 2009/02/13, https://doi.org/10.1007/s10544-009-9286-819212816.

[57] Miller PG, Shuler ML. Design and demonstration of a pumpless 14 compartment microphysiological system. Biotechnol Bioeng 2016;113(10):2213–27. https://doi.org/10.1002/bit.25989.
[58] Ghanem A, Shuler ML. Combining cell culture analogue reactor designs and PBPK models to probe mechanisms of naphthalene toxicity. Biotechnol Prog 2000;16(3):334–45. Epub 2000/06/03, https://doi.org/10.1021/bp990152210835232.
[59] Viravaidya K, Shuler ML. Incorporation of 3T3-L1 cells to mimic bioaccumulation in a microscale cell culture analog device for toxicity studies. Biotechnol Prog 2004;20(2):590–7. Epub 2004/04/03, https://doi.org/10.1021/bp034238d15059006.
[60] Van Kuilenburg ABP, Meinsma R, Zoetekouw L, Van Gennip AH. Increased risk of grade IV neutropenia after administration of 5-fluorouracil due to a dihydropyrimidine dehydrogenase deficiency: high prevalence of the IVS14+1g>a mutation. Int J Cancer 2002;101(3):253–8. https://doi.org/10.1002/ijc.10599.
[61] Esch MB, Smith AST, Prot J-M, Oleaga C, Hickman JJ, Shuler ML. How multi-organ microdevices can help foster drug development. Adv Drug Deliv Rev 2014;69–70:158–69. https://doi.org/10.1016/j.addr.2013.12.003.
[62] Sakolish CM, Esch MB, Hickman JJ, Shuler ML, Mahler GJ. Modeling barrier tissues in vitro: methods, achievements, and challenges. EBioMedicine 2016;5:30–9. https://doi.org/10.1016/j.ebiom.2016.02.023.
[63] Bauer S, Wennberg Huldt C, Kanebratt KP, Durieux I, Gunne D, Andersson S, et al. Functional coupling of human pancreatic islets and liver spheroids on-a-chip: towards a novel human ex vivo type 2 diabetes model. Sci Rep 2017;7(1):14620. Epub 2017/11/04, https://doi.org/10.1038/s41598-017-14815-w29097671.
[64] Maschmeyer I, Lorenz AK, Schimek K, Hasenberg T, Ramme AP, Hubner J, et al. A four-organ-chip for interconnected long-term co-culture of human intestine, liver, skin and kidney equivalents. Lab Chip 2015;15(12):2688–99. Epub 2015/05/23, https://doi.org/10.1039/c5lc00392j25996126.
[65] Yoon DY, Mansukhani NA, Stubbs VC, Helenowski IB, Woodruff TK, Kibbe MR. Sex bias exists in basic science and translational surgical research. Surgery 2014;156(3):508–16. Epub 2014/09/02, https://doi.org/10.1016/j.surg.2014.07.00125175501.
[66] Vunjak-Novakovic G, Bhatia S, Chen C, Hirschi K. HeLiVa platform: integrated heart-liver-vascular systems for drug testing in human health and disease. Stem Cell Res Ther 2013;4(1):S8. https://doi.org/10.1186/scrt369.
[67] Price PS, Conolly RB, Chaisson CF, Gross EA, Young JS, Mathis ET, et al. Modeling interindividual variation in physiological factors used in PBPK models of humans. Crit Rev Toxicol 2003;33(5):469–503. Epub 2003/11/05, 14594104.
[68] Trietsch SJ, Israels GD, Joore J, Hankemeier T, Vulto P. Microfluidic titer plate for stratified 3D cell culture. Lab Chip 2013;13(18):3548–54. Epub 2013/07/28, https://doi.org/10.1039/c3lc50210d23887749.
[69] Wilmer MJ, Ng CP, Lanz HL, Vulto P, Suter-Dick L, Masereeuw R. Kidney-on-a-chip technology for drug-induced nephrotoxicity screening. Trends Biotechnol 2016;34(2):156–70. Epub 2015/12/29, https://doi.org/10.1016/j.tibtech.2015.11.00126708346.
[70] Esch MB, Prot J-M, Wang YI, Miller P, Llamas-Vidales JR, Naughton BA, et al. Multi-cellular 3D human primary liver cell culture elevates metabolic activity under fluidic flow. Lab Chip 2015;15(10):2269–77. https://doi.org/10.1039/c5lc00237k.
[71] Zhang B, Radisic M. Organ-on-a-chip devices advance to market. Lab Chip 2017;17(14):2395–420. Epub 2017/06/16, https://doi.org/10.1039/c6lc01554a28617487.